

Spectra of non-hermitian quantum spin chains describing boundary induced phase transitions

Ulrich Bilstein[‡] and Birgit Wehefritz[§]

*Universität Bonn, Physikalisches Institut
Nußallee 12, D-53115 Bonn, Germany*

Abstract

The spectrum of the non-hermitian asymmetric XXZ-chain with additional non-diagonal boundary terms is studied. The lowest lying eigenvalues are determined numerically. For the ferromagnetic and completely asymmetric chain that corresponds to a reaction-diffusion model with input and outflow of particles the smallest energy gap corresponding directly to the inverse of the temporal correlation length shows the same properties as the spatial correlation length of the stationary state. For the antiferromagnetic chain with both boundary terms, we find a conformal invariant spectrum where the partition function corresponds to the one of a Coulomb gas with only magnetic charges shifted by a purely imaginary and a lattice-length dependent constant. Similar results are obtained by studying a toy model that can be diagonalized analytically in terms of free fermions.

PACS numbers: 05.70.Ln, 64.60.Ht, 64.90.+b, 75.10.Jm

[‡] bilstein@theo1.physik.uni-bonn.de

[§] birgit@theo1.physik.uni-bonn.de

1. Introduction

In the study of reaction-diffusion processes non-hermitian chains appear in a natural way. However, their properties have not yet been studied extensively. For instance, the effect of boundary conditions on the spectrum of non-hermitian Hamiltonians is unknown, although a rich and surprising structure arises here. In this article we study an asymmetric XXZ-chain with modified boundary terms and we show that these boundary terms give rise to new and interesting features.

In this article, two examples are treated that both show the appearance of boundary-induced phase transitions. As a first example, we study the Hamiltonian of the asymmetric diffusion model on a one-dimensional lattice with open boundaries, injection and ejection of particles at the edges of the chain. For this model, all known results are valid only for the stationary state. The time evolution is studied for the first time in this article. In this model, particles of one species can diffuse on the lattice with length N with a rate p to the right and q to the left. Particles are injected at the left boundary with a rate α and extracted with a rate β at the right boundary. The Hamiltonian of this model is non-hermitian and is given by the following expression:

$$H = - \sum_{j=1}^{N-1} \left[q\sigma_j^- \sigma_{j+1}^+ + p\sigma_j^+ \sigma_{j+1}^- + \frac{p+q}{4}(\sigma_j^z \sigma_{j+1}^z - 1) + \frac{q-p}{4}(\sigma_{j+1}^z - \sigma_j^z) \right] + B_1 + B_N \quad (1.1)$$

with

$$\begin{aligned} B_1 &= \frac{\alpha}{2}(\sigma_1^z - 2\sigma_1^- + 1) \\ B_N &= -\frac{\beta}{2}(\sigma_N^z + 2\sigma_N^+ - 1) \end{aligned} \quad (1.2)$$

The bulk term of this Hamiltonian corresponds to the asymmetric XXZ-Hamiltonian with anisotropy $\Delta = \frac{p+q}{2}$. This model and versions of it have been studied extensively. The total asymmetric diffusion model (with $q = 0$) was first defined by Derrida, Domany and Mukamel [1] who found the phase diagram for the current in the stationary state as a function of α and β by application of mean-field theory. The ground state of the model can be determined exactly by a matrix product formulation [2, 3]. Two massive and one massless phase have been found for different regions of the α - β plane. The massive phases are separated by a line on which the spectrum is massless. In this context massless means that the spatial correlation length diverges, which implies an algebraic falloff of the spatial concentration profile. On the other hand, massive means that the spatial correlation length remains finite. The phase diagram for the partially asymmetric system ($p \neq q \neq 0$) was presented for the first time in [4]. Essler and Rittenberg [5] calculated correlation functions for this system with the help of the matrix product formulation.

The case of periodic boundary conditions has previously been studied by Gwa and Spohn [6] for $q = 0$ and $p = 1$ using Bethe-Ansatz techniques; for arbitrary values of p and q , results

can be found in [7, 8].

The first part of this article deals with the analysis of the spectrum of H for $q = 0$. The Hamiltonian is known to be integrable [9], but because of the lack of a reference state, the model cannot be treated by a Bethe-Ansatz. Therefore numerical methods are applied here. We were interested in determining the correspondence between the spatial correlation lengths already known from previous work described above and the dynamical properties of the Hamiltonian, i. e. the time correlation length τ given by the inverse of the smallest energy gap E_G with respect to the ground state of the Hamiltonian [10]. E_G is determined for lattice lengths of $2 \leq N \leq 18$ sites and then extrapolated to the thermodynamical limit. We find that τ remains finite in the massive phase and diverges algebraically in the massless regime. The boundary induced phase diagram known for the stationary state is reproduced by the spectrum of the Hamiltonian; so the dynamics of the system exhibits the same physical properties as the stationary state.

The second part of the paper is devoted to the antiferromagnetic version of the Hamiltonian $-H$ where H was mentioned above. It can no longer be interpreted as Hamiltonian of a reaction-diffusion system, but nevertheless it describes interesting physical models, e.g. imposing periodic boundary conditions it can be viewed as the logarithmic derivative of the transfer matrix of the six-vertex model [11] and it can be used to describe the equilibrium shape of a crystal [12] or a surface growth model [13]. The phase diagram of the antiferromagnetic chain with periodic boundary conditions has been determined recently [14]. A natural question arises whether different boundary terms alter the phase diagram in such a way that boundary induced phase transitions occur and indeed this phenomenon can be found again. It manifests itself clearly in the study of the partition function of the system. Before presenting our examples we give the definition of the partition functions we are going to use. For periodical systems the partition function is given by

$$\mathcal{Z} = \lim_{N \rightarrow \infty} \text{tr}_Z \frac{N}{2\pi\xi} (H - e_\infty N) \quad (1.3)$$

for open systems by

$$\mathcal{Z} = \lim_{N \rightarrow \infty} \text{tr}_Z \frac{N}{\pi\xi} (H - f_\infty - e_\infty N) \quad (1.4)$$

Here ξ is a normalization constant, e_∞ the bulk free energy and f_∞ the surface free energy. For a comparison with the results for the asymmetric XXZ chain let us first repeat some known results for the symmetric XXZ-chain with different (but not lattice-length dependent) boundary conditions. It has been studied extensively by using numerical and analytical methods (Bethe-Ansatz) [15, 16]. In the regime $-1 \leq \Delta < 1$ the spectrum is massless and can be described by a representation of the Virasoro algebra with central charge $c = 1$. The partition function corresponds exactly to the one of a Coulomb gas with electric charges n and magnetic charges m [17] where n corresponds to the total spin of the chain. It can also be described by a Gaussian field theory with compactification radius R [18]. It is given by

the following expression (using an appropriate normalization $\xi(\Delta)$):

$$\mathcal{Z} = z^{-\frac{1}{12}} \sum_{m \in \mathbb{Z}, n} z^{\frac{1}{2}(\frac{n^2}{R^2} + R^2 m^2)} \Pi_V^2(z) \quad (1.5)$$

with

$$\Pi_V(z) = \prod_{i=1}^{\infty} (1 - z^i)^{-1} \quad . \quad (1.6)$$

In eq. (1.5) n takes integer values for an even number of sites and half-integer values for an odd number of sites.

The spectrum of the chain without any boundary terms is given by a Coulomb gas with only electric charges n . Here the partition function reads [15]

$$\mathcal{Z} = z^{-\frac{1}{24}} \sum_{n \in \frac{\mathbb{Z}}{2}} z^{\frac{n^2}{R^2}} \Pi_V(z) \quad (1.7)$$

This expression is valid for the open symmetric XXZ-chain as well as for the open asymmetric XXZ-chain since there exists a mapping of the symmetric onto the asymmetric XXZ-chain.

For the periodic asymmetric XXZ-chain that is normally massive in the antiferromagnetic region, a massless phase was found for $\Delta < 1$ [8, 14]. Here the operator content contains a term which is proportional to the lattice length N so that the partition function is the one of a modified Coulomb gas. It has been calculated by Noh and Kim using Bethe-Ansatz calculations [8].

$$\mathcal{Z} = z^{-\frac{1}{12}} \sum_{m \in \mathbb{Z}, n} z^{\frac{1}{2}(\frac{n^2}{R^2} + R^2 m^2 + 2imNy)} \Pi_V^2(z) \quad (1.8)$$

The compactification radius R depends on Δ and q/p , n takes integer values for even lattice lengths and half-integer values for odd lattice lengths.

These three examples show that boundary conditions can change the spectrum of the asymmetric XXZ-chain drastically.

The boundary conditions we analyse in this article (with additional non-diagonal boundary terms) have not been treated before. Our new results are obtained by determining the lowest-lying eigenvalues of the Hamiltonian up to 18 sites in the general case and 21 sites in the CP-invariant case ($\alpha = \beta$). As the Hamiltonian does not have any symmetries in the general case and is non-hermitian, the diagonalization requires a large amount of CPU-time. A version of the deflated Arnoldi algorithm has been applied to quantum spin chains for the first time here. The Arnoldi algorithm that reduces to the Lanczos algorithm in the case of hermitian matrices was already used for the determination of the spectrum of the Potts model [19]. Another example where a non-hermitian chain was treated numerically can be found in [20].

The analysis of the spectrum for $p > q$ and $\alpha, \beta > 0$ suggests surprisingly the partition function of a Coulomb gas that has only magnetic charges. Additionally, the magnetic

quantum number m is shifted by an imaginary amount ix .

$$\mathcal{Z} = z^{-\frac{1}{24}} \sum_{m \in \frac{\mathbb{Z}}{2}} z^{R^2(m+i(x+Ny))^2} \Pi_V(z) \quad (1.9)$$

Here $x = x(\frac{q}{p}, \frac{\alpha}{p}, \frac{\beta}{p})$ and $y = y(\frac{q}{p})$. For even lattice lengths m takes half-integer values, for odd lattice lengths integer values. The spectrum is given by non-unitary representations of the $U(1)$ Kac-Moody algebra. For $q = 0$ the parameters y and R correspond exactly to the ones that appear for the periodic system [6]. The term proportional to x however is caused by the boundary terms alone. For $\alpha\beta = 0$ the spectrum is massive, so we can conclude that the boundary terms give rise to the conformal invariant structure of the spectrum.

We also studied a toy model consisting of a simplified version of the Hamiltonian (1.1) that can be diagonalized in terms of free fermions. The properties of the spectra that have been found numerically can be found again in the analytical results for the toy model. Additionally, we gain some insight into the role the different boundary terms play for the spectrum of the Hamiltonian.

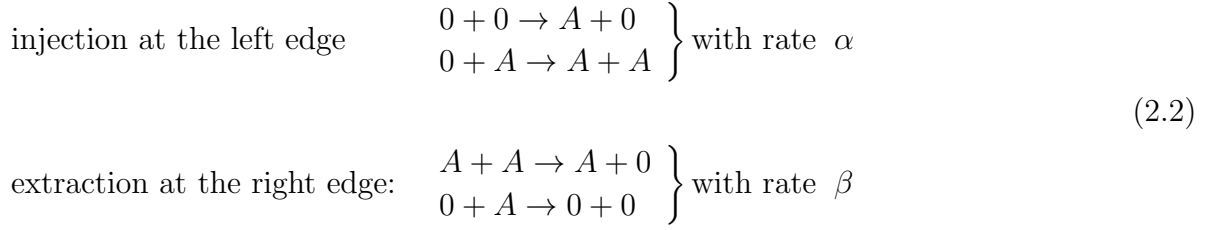
The article is organized as follows: In the first part, we define the total asymmetric diffusion model with open boundaries and additional injection and extraction terms. We present our numerical results for the temporal correlation length in the second part and compare them to the phase diagram of the stationary state and the known expressions for spatial correlation lengths. The third part deals with the antiferromagnetic version of the Hamiltonian. From the finite-size scaling behaviour of the lowest-lying energy levels we conclude the form of the partition function (1.9). The fourth part describes analytical results obtained by diagonalization of the toy model for non-hermitian boundary conditions. Here the characteristic properties of the Hamiltonian that has been treated numerically are reproduced, thus the calculations for the simplified model give similar results to our numerical analysis of the more complicated model. We close with a discussion of our results. In the appendix tables of the numerical results of the second and third part can be found.

2. Asymmetric diffusion model with boundary terms

We consider a model defined on a chain with N sites. Each site can be either occupied by a particle of species A or empty. For the dynamics, we consider only processes that involve two neighbouring sites. The following processes are allowed:

$$\begin{aligned} \text{diffusion to the right: } & A + 0 \rightarrow 0 + A && \text{with rate } p \\ \text{diffusion to the left: } & 0 + A \rightarrow A + 0 && \text{with rate } q \end{aligned} \quad (2.1)$$

Additionally, we allow processes that occur only at the two edges of the chain:



To each site j of the chain we attach a variable γ_j that takes the value 1 if the site is occupied by a particle and 0 if the site is empty. A configuration of the model is described by a set of variables $\{\gamma\} = \{\gamma_1, \gamma_2, \dots, \gamma_N\}$. The probability that a state (μ, ν) on two adjacent sites will change into the state (ρ, σ) after one unit of time is denoted by:

$$\Gamma_{\rho, \sigma}^{\mu, \nu}; \quad (\mu, \nu) \neq (\rho, \sigma). \tag{2.3}$$

All reactions changing the state (μ, ν) into any other state are summarized in the rate $\Gamma_{\mu, \nu}$:

$$\Gamma_{\mu, \nu} = \sum'_{\rho, \sigma=0} \Gamma_{\rho, \sigma}^{\mu, \nu}, \tag{2.4}$$

where the prime is always used to indicate that in the sum the case $(\rho, \sigma) = (\mu, \nu)$ is excluded. This definition ensures the conservation of probabilities.

The dynamics of the system is given by the time evolution of the probability $P(\{\gamma\}, t)$ to find the system in the configuration $\{\gamma\}$ at time t . The time evolution is described by the master equation [21]

$$\begin{aligned}
\frac{\partial}{\partial t} P(\{\gamma\}; t) &= \sum_{k=1}^{L-1} \left[-\Gamma_{\gamma_k, \gamma_{k+1}} P(\gamma_1, \dots, \gamma_L; t) \right. \\
&\quad \left. + \sum_{\delta_k, \delta_{k+1}=0}^1 \Gamma_{\gamma_k, \gamma_{k+1}}^{\delta_k, \delta_{k+1}} P(\gamma_1, \dots, \gamma_{k-1}, \delta_k, \delta_{k+1}, \gamma_{k+2}, \dots, \gamma_L; t) \right].
\end{aligned} \tag{2.5}$$

The master equation can be mapped on a Euclidean Schrödinger equation. For this purpose, one defines a ket vector describing the probability distribution in a 2^N dimensional vector space $C^{\otimes N}$:

$$|P(t)\rangle = \sum_{\{\gamma\}} P(\{\gamma\}, t) |\{\gamma\}\rangle. \tag{2.6}$$

The master equation then takes the form

$$\frac{\partial}{\partial t} |P(t)\rangle = -H |P(t)\rangle. \tag{2.7}$$

where the Hamiltonian is a sum of nearest neighbor terms

$$H = \sum_{k=1}^{N-1} H_{k, k+1} \tag{2.8}$$

The 4×4 matrices $H_{k,k+1}$ are given by the following expression with respect to the basis of states $|11\rangle, |10\rangle, |01\rangle, |00\rangle$

$$H_{k,k+1} = \begin{pmatrix} 0 & 0 & 0 & 0 \\ 0 & q & -p & 0 \\ 0 & -q & p & 0 \\ 0 & 0 & 0 & 0 \end{pmatrix} \quad \text{for } k = 2, 3, \dots, N-2 \quad . \quad (2.9)$$

The boundary terms which arise due to the processes of injection on the first lattice site and extraction on the last site can be written in this formalism as

$$H_{1,2} = \begin{pmatrix} \alpha & 0 & 0 & 0 \\ 0 & q + \alpha & -p & 0 \\ -\alpha & -q & p & 0 \\ 0 & -\alpha & 0 & 0 \end{pmatrix}, \quad H_{N-1,N} = \begin{pmatrix} 0 & -\beta & 0 & 0 \\ 0 & q + \beta & -p & 0 \\ 0 & -q & p & -\beta \\ 0 & 0 & 0 & \beta \end{pmatrix}. \quad (2.10)$$

The Hamiltonian can also be expressed in terms of Pauli spin matrices σ^x, σ^y and σ^z :

$$H = - \sum_{j=1}^{L-1} \left[q\sigma_j^- \sigma_{j+1}^+ + p\sigma_j^+ \sigma_{j+1}^- + \frac{p+q}{4}(\sigma_j^z \sigma_{j+1}^z - 1) + \frac{q-p}{4}(\sigma_{j+1}^z - \sigma_j^z) \right] + B_1 + B_N \quad (2.11)$$

with boundary terms

$$B_1 = \frac{\alpha}{2}(\sigma_1^z - 2\sigma_1^- + 1) \quad , \quad B_N = -\frac{\beta}{2}(\sigma_N^z + 2\sigma_N^+ - 1) \quad . \quad (2.12)$$

The spectrum of H stays invariant if α and β are permuted. This permutation can be obtained on the level of the Hamiltonian by applying the similarity transformation $\sigma^\pm \rightarrow \sigma^\mp, \sigma^z \rightarrow -\sigma^z$ and a simultaneous reflection of the system. Physically one can understand this property by denoting that particle-hole symmetry holds: The model can be seen as describing particles moving in one direction or holes moving in the opposite direction. If $\alpha = \beta$, the Hamiltonian is invariant under this transformation (CP -symmetry).

The Hamiltonian can also be mapped by a unitary transformation U onto the symmetric XXZ-chain with different boundary terms. This correspondence will prove very helpful in the sequel and therefore it will be given explicitly here. If we take

$$U = \prod_{j=1}^N U_j \quad , \quad U_j = I_1 \otimes \dots \otimes I_{j-1} \otimes \begin{pmatrix} 1 & 0 \\ 0 & \Lambda \mathcal{Q}^{j-1} \end{pmatrix} \otimes I_{j+1} \otimes \dots \otimes I_N \quad (2.13)$$

with $\mathcal{Q} = \sqrt{\frac{q}{p}}$ and arbitrary Λ the transformed Hamiltonian $H' = UHU^{-1}$ is:

$$H' = -\frac{\sqrt{pq}}{2} \sum_{j=1}^{N-1} \left[\sigma_j^x \sigma_{j+1}^x + \sigma_j^y \sigma_{j+1}^y + \frac{\mathcal{Q} + \mathcal{Q}^{-1}}{2}(\sigma_j^z \sigma_{j+1}^z - 1) \right]$$

$$+\frac{\mathcal{Q}-\mathcal{Q}^{-1}}{2}(\sigma_{j+1}^z-\sigma_j^z)\Big]+B'_1+B'_N\quad . \quad (2.14)$$

This is the $U_{\mathcal{Q}}SU(2)$ invariant Hamiltonian [22] with additional length-dependent boundary terms:

$$\begin{aligned} B'_1 &= \frac{\alpha}{2}(\sigma_1^z - 2\mathcal{Q}^{\frac{1-N}{2}}\sigma_1^- + 1) \quad , \\ B'_N &= -\frac{\beta}{2}(\sigma_N^z + 2\mathcal{Q}^{\frac{1-N}{2}}\sigma_N^+ - 1) \quad . \end{aligned} \quad (2.15)$$

Although this Hamiltonian is known to be integrable [9], it cannot be solved by the Bethe-Ansatz because one cannot construct a reference state. The non-hermitian boundary terms induce completely different properties of the Hamiltonian H in comparison to H' without B'_1 and B'_2 . The reason for this can be understood by considering the matrix form of H . As the bulk terms (without B'_1 and B'_2) commute with the total spin $S^z = \sum_{j=1}^N \sigma_j^z$, these bulk terms can be written as a matrix in block-diagonal form, where each block operates in a sector with fixed total spin. The boundary terms change the total spin by ± 1 , so they will appear in blocks below or above the diagonal. Only in the case where $\alpha \neq 0$ **and** $\beta \neq 0$, they will give contributions to the spectrum. In all other cases the spectrum of H is the massive spectrum of the $U_{\mathcal{Q}}SU(2)$ -invariant XXZ-chain.

3. Results for the total asymmetric diffusion model with boundary terms

3.1. Analytical results for the stationary state

For future reference, let us first present some of the results achieved previously for the total asymmetric diffusion model. Up to now, all results are known for the stationary state. In [3] the phase diagram for the current and the spatial profile of the concentration have been determined as functions of α and β . The current through the bond j for the configuration γ is defined as:

$$j_k = \sum_{\{\gamma\}} \gamma_k(1 - \gamma_{k+1})P(\{\gamma\}, t) \quad . \quad (3.1)$$

The phase diagram is given in figure 1. There are three main phases, characterized by the density of particles: The high-density phase A , the low-density phase B and the maximal current phase C . Phases A and B are further subdivided into A_1, A_2 and B_1, B_2 . Phases A and B are separated by a line which is called 'coexistence line'. In the thermodynamic limit, the currents in the three phases are given by:

$$\begin{aligned} A &: \quad j = \beta(1 - \beta) \\ B &: \quad j = \alpha(1 - \alpha) \quad . \end{aligned} \quad (3.2)$$

$$C \quad : \quad j = \frac{1}{4}$$

The density profile of the concentration on the stationary state obtained in [3] allows to read off the spatial correlation length ξ in the different phases. In the phase A , ξ is defined by

$$\langle n_k \rangle = \text{const.} + \text{const.} \exp(-k/\xi) \quad ; \quad (3.3)$$

in the phase B it is given by

$$\langle n_k \rangle = \text{const.} + \text{const.} \exp\left(\frac{k - N - 1}{\xi}\right) \quad . \quad (3.4)$$

In the different phases the expressions for the correlation length are:

$$\begin{aligned} A_1 : \xi &= \left(\ln\left(\frac{\alpha(1-\alpha)}{\beta(1-\beta)}\right) \right)^{-1} \\ A_2 : \xi &= -\ln(4\beta(1-\beta)) \\ B_1 : \xi &= \left[\ln\left(\frac{\beta(1-\beta)}{\alpha(1-\alpha)}\right) \right]^{-1} \\ B_2 : \xi &= -\ln(4\alpha(1-\alpha)) \end{aligned} \quad (3.5)$$

In the phase C and on the coexistence line the one-point function $\langle n_k \rangle$ shows an algebraic behaviour:

$$\begin{aligned} C : \langle n_{N-k} \rangle &= \frac{1}{2} - \frac{1 - \delta_{\beta, \frac{1}{2}}}{2\sqrt{\pi}} k^{-\frac{1}{2}} \\ \text{coexistence line} : \langle n_k \rangle &= \alpha + k \frac{1 - 2\alpha}{N} \end{aligned} \quad (3.6)$$

3.2. Numerical results for the time correlation length

In this chapter we compare the phase structure of the stationary state to the spectrum of the Hamiltonian. We investigate the gap between the ground state and the first excited state of the spin chain. This energy gap E_G allows us to read off the time correlation length τ directly:

$$\tau^{-1} \simeq E_G \quad . \quad (3.7)$$

We determine the lowest lying excitation energies for lattice lengths $2 \leq N \leq 18$ by diagonalizing the Hamiltonian numerically, using a version of the deflated Arnoldi algorithm [23] that reduces to the Lancos algorithm in the case of hermitian matrices. The eigenvalues were then extrapolated with the help of the BST-algorithm [24]. α and β have been varied in steps of 0.1 between 0.1 and 1. The following form of the energy gap has been found in the different regions of the phase diagram. In the phases A_1 and B_1 , E_G is a function of α and β , while in phase B_2 , E_G depends only on α and in phase A_2 only on β . In phase C and on

the coexistence line the system is massless:

$$\begin{aligned}
A_1 & : & E_G &= m(\alpha, \beta) \\
A_2 & : & E_G &= m(\beta) \\
B_1 & : & E_G &= m(\alpha, \beta) \\
B_2 & : & E_G &= m(\alpha) \\
C & : & E_G &\sim N^{-\frac{3}{2}} \\
\alpha = \beta < \frac{1}{2} & : & E_G &\sim N^{-2}
\end{aligned} \tag{3.8}$$

Here m denotes the mass of the spectrum.

Table I shows extrapolants for the energy gaps. One sees clearly that in the phase B_1 the energy gap depends on both α and β while it depends only on α in the phase B_2 . We did not give any extrapolants for the phases A_1 and A_2 since the spectrum is symmetric under permutation of α and β as described in section 2. Table I also shows that the mass gap vanishes in the phase C and on the coexistence line. In Table II extrapolants for the exponent $\frac{3}{2}$ in the phase C and for the exponent 2 on the coexistence line can be found.

Comparing these results with (3.5-3.6), we can see that the temporal correlation length shows the same behaviour as the spatial correlation length in the different phases: in the phase C and on the coexistence line τ diverges algebraically while it remains finite in the phases A and B . The exponent $\frac{3}{2}$ has also been found for the total asymmetric diffusion model with periodic boundary conditions [6]. The exponent 2 was found for the symmetric XXZ chain with periodic boundary conditions at the point $\Delta = 1$. The periodic model can be mapped onto a model for surface growth [6, 7, 25]. This mapping can be formulated analogously for the open chain with additional boundary terms that is treated here. Then, in the language of growth models, the exponent $\frac{3}{2}$ describes KPZ-type growth [26] while the exponent 2 corresponds to Edwards-Wilkinson growth behaviour [13]. In phases A_2 and B_2 τ depends only on β or α respectively. However, the numerical values for the temporal correlation length are different from the ones for the spatial correlation length. The fact that the temporal evolution of the system reflects itself in the stationary state (for $t \rightarrow \infty$) is not yet understood. This is not true in general, as there are examples for a different behaviour of the spatial and the temporal correlation length [27]. However, in this case it is a striking and unexpected feature that shows how strong boundary conditions change the properties of non-hermitian quantum chains.

4. The antiferromagnetic chain

In the following, we will treat the antiferromagnetic Hamiltonian which can be obtained from the ferromagnetic one (that has been treated before) by applying a similarity transformation. As has been shown in chapter 2 the ferromagnetic chain can be connected to a XXZ-chain

with anisotropy $\Delta = \frac{p+q}{2} \geq 1$. The antiferromagnetic chain corresponds to $\Delta \leq 1$ and can be written as

$$H'' = - \sum_{j=1}^{L-1} \left[q\sigma_j^- \sigma_{j+1}^+ + p\sigma_j^+ \sigma_{j+1}^- - \frac{p+q}{4}(\sigma_j^z \sigma_{j+1}^z - 1) - \frac{q-p}{4}(\sigma_{j+1}^z - \sigma_j^z) \right] + B_1'' + B_N''$$

with boundary terms

$$\begin{aligned} B_1'' &= -\frac{\alpha}{2}(\sigma_1^z + 2\sigma_1^- + 1) \quad , \\ B_N'' &= \frac{\beta}{2}(\sigma_N^z + (-1)^N 2\sigma_N^+ - 1) \quad . \end{aligned} \tag{4.1}$$

Due to the minus sign in the transformation rule, the low lying excitations of the ferromagnetic chain correspond to the highest states of the antiferromagnetic chain and vice versa.

The numerical studies concentrate on the case $q = 0$ and $p = 1$ with $\alpha, \beta \geq 0$. For this choice of parameters the extrapolated values converge very well.

The analysis of the spectrum reveals that it is conformal invariant. We studied the finite-size scaling behaviour of the model in order to determine the operator content of the underlying conformal field theory. For conformal invariant systems, the ground state is supposed to take the following form for finite lattices and for periodic boundary conditions [28, 29]

$$\frac{E_0(N)}{N} = e_\infty - \frac{\pi\xi c}{6N^2} - o(N^{-2}) \tag{4.2}$$

The excited state E_r satisfies [30]

$$\mathcal{E}_r = \lim_{N \rightarrow \infty} \frac{N}{2\pi\xi} (E_r(N) - E_0(N)) = (\Delta + r) + (\bar{\Delta} + \bar{r}) \quad ; \tag{4.3}$$

for open boundary conditions, one gets an additional surface term f_∞ in the ground state energy [31]:

$$\frac{E_0(N)}{N} = e_\infty + \frac{f_\infty}{N} - \frac{\pi\xi c}{24N^2} - o(N^{-2}) \quad . \tag{4.4}$$

The energy gaps scale here as

$$\mathcal{E}_r = \lim_{N \rightarrow \infty} \frac{N}{\pi\xi} (E_r(N) - E_0(N)) = (\Delta + r) \quad ; \tag{4.5}$$

Here ξ is a normalization constant, c the central charge of the Virasoro algebra.

In our case, the spectrum had to be treated separately for even and odd lattice lengths. Since the ground state was calculated for an odd number of sites, we used interpolated values from odd lattice lengths for the values of the ground state for even lattice lengths. While the ground state energy is real for all lattice lengths, most of the excited states have a

non-vanishing imaginary part. This is a feature that did already appear for the periodic asymmetric XXZ chain [8] and in the calculation of the operator content of the five vertex model defined on an anisotropic lattice [32].

We considered the imaginary part of the energy gap

$$\mathcal{I} = \lim_{N \rightarrow \infty} \frac{1}{\pi\xi} \text{Im}(E(N)) \quad , \quad (4.6)$$

the correction to the real part

$$\text{Re}(\mathcal{E}) = \lim_{N \rightarrow \infty} \frac{N}{\pi\xi} \text{Re}(E(N) - E_0(N)) \quad (4.7)$$

and the correction to the imaginary part

$$\text{Im}(\mathcal{E}) = \lim_{N \rightarrow \infty} \frac{N}{\pi\xi} \text{Im}(E(N) - \mathcal{I}) \quad (4.8)$$

The data reveals the following finite-size scaling behaviour for the normalized eigenvalues:

$$\frac{N}{\pi\xi} (E_r^m - E'_0) = R^2 (m + i(x + yN))^2 + r \quad , \quad r \in N \quad , \quad (4.9)$$

and the ground state behaves as

$$E'_0 = E_0 + \pi\xi \left(\frac{R^2}{N} (x + yN)^2 \right) \quad . \quad (4.10)$$

Here m is a quantized number and takes for odd lattice lengths the integer values $m = 0, \pm 1, \pm 2, \dots$, for even lattice lengths half-integer values $m = \pm \frac{1}{2}, \pm \frac{3}{2}, \dots$. The precise relation between the extrapolants and the constants R, x and y is given by:

$$\begin{aligned} \mathcal{I}_r^m &= 2R^2 m y, \\ \text{Re}(\mathcal{E}_r^m) &= R^2 m^2 + r, \\ \text{Im}(\mathcal{E}_r^m) &= 2R^2 m x. \end{aligned} \quad (4.11)$$

Data for $r = 0$ is shown in table III. As H is real, we find for each complex eigenvalue E also the complex conjugate E^* . Therefore all tables only show data for $m \geq 0$. Data for $r \geq 0$ can be found in table IV for $m = 0$ and $m = \frac{1}{2}$. The corresponding data for $m = 1, \frac{3}{2}, 2, \frac{5}{2}$ and 3 has also been obtained.

The next constant that has to be determined is the conformal charge c' . The ground state energy in the thermodynamic limit, e_∞ , is already known from the periodical system. The surface energy f_∞ can be obtained by extrapolation of

$$f_\infty = \lim_{N \rightarrow \infty} (E_0(N) - N e_\infty) \quad . \quad (4.12)$$

The results are given in table V. Now c can be obtained via

$$c = \lim_{N \rightarrow \infty} \frac{24N}{\pi\xi} (E_0(N) - N e_\infty - f_\infty) \quad . \quad (4.13)$$

The numerical values for c are not constant for different values of α and β (see table VI). However, we can shift all energy gaps, independently of the sector by a constant term $24R^2x(\alpha, \beta)^2$ that depends on α and β (table VII). Absorbing this shift into the ground state, one can define a new central charge c'

$$c' = c - 24R^2x^2 \quad . \quad (4.14)$$

which is indeed constant within the numerical errors. The numerical values show an excellent agreement with $c' = 1$ (table VI).

The term $\pi\xi I_r^m$, the imaginary part of the energy gaps, takes (independently of α and β) for odd lattice lengths multiples of the same constant 1.8854... that already appeared in the calculation of Gwa and Spohn [6] for the periodic system as imaginary part of the smallest energy gap. Using Bethe Ansatz calculations for the first and second smallest eigenvalue in the sector with spin 0 they obtained the following result

$$e_\infty = 0.690140115. \quad (4.15)$$

$$(E_1 - E_0)_{per} = 6.5776787N^{-1} + i1.885456427. \quad (4.16)$$

This result can be used to obtain estimates for the parameters R and y , if one assumes that also the spectrum of the periodic chain is characterized by these parameters, and the finite-size scaling of the lowest lying state with spin 0 is given by [8]

$$\frac{N}{2\pi\xi}(E_1 - E_0)_{per} = \frac{1}{2}R^2 + iR^2yN \quad . \quad (4.17)$$

The estimates that have been obtained using this assumption can now be compared to the numerical results. Tables III and IV show a comparison between the values obtained from the analytical calculation and the numerical results. The normalization constant ξ has been taken from numerical Bethe Ansatz calculations for the periodical system for up to 80 sites [33]:

$$\xi = 1.64784392694623 \quad . \quad (4.18)$$

The data shows that indeed the periodic system is characterized by the same parameters as the open system with additional boundary terms. However, the full operator content of the two chains is different. This effect comes from the different boundary terms only.

The degeneracies of the energy levels for $r = \text{const.}$ are described by the characterfunction of a $U(1)$ Kac-Moody algebra [34]. This confirms the above result $c' = 1$. The Kac-Moody algebra is defined by its commutation relations

$$[T_m, T_n] = m\delta_{m+n,0} \quad , \quad m, n \in Z \quad . \quad (4.19)$$

The character function is given by

$$\chi_{\Delta,q}(z, y) = \text{tr}(z^{L_0}y^{T_0}) = z^{\frac{q^2}{2}}\Pi_V(z)y^q \quad . \quad (4.20)$$

where L_0 is a generator of the Virasoro algebra with conformal weight $c = 1$ that can be canonically obtained from the $U(1)$ Kac-Moody algebra using the Sugawara construction [35]. Here q is the eigenvalue of T_0 , and the highest weight representation is $[\Delta, q]$. A shift in the algebra characterized by a parameter φ

$$\tilde{T}_m = T_m + \varphi \delta_{m,0} \quad (4.21)$$

does not change the commutation relations above but leads to a representation with highest weights

$$\tilde{\Delta} = \frac{1}{2} \tilde{q}^2 \quad \text{where} \quad \tilde{q} = q + \varphi \quad (4.22)$$

If φ is chosen to be complex, one obtains a representation of the Kac-Moody algebra with negative conformal dimensions. In this case however $\tilde{T}_0^+ \neq \tilde{T}_0^-$ and the representation is not unitary.

In our case, the part of the energy corrections that is independent of N can be described by a non-unitary representation of a shifted Kac-Moody algebra. The parameter x depends on the boundary terms. The shift φ of the Kac-Moody algebra is given by $\varphi = \sqrt{2}i(x + Ny)$.

The results for the antiferromagnetic chain can be summarized in the partition function

$$\mathcal{Z} = z^{-\frac{1}{24}} \sum_{m \in \frac{\mathbb{Z}}{2}} z^{R^2(m+i(x+Ny))^2} \Pi_V(z) \quad (4.23)$$

The operator content of this model corresponds to the one of a Coulomb gas with only magnetic charges and an additional term that depends on the lattice length N . All calculations for $q \neq 0 \neq p$ for $p > q$ show similar results but reveal that in this case x and y are functions of the ratio q/p .

The case $q > p$ has not been studied systematically. Here the spectra are purely real, but the convergence of the extrapolations is too bad to obtain precise estimates (the same holds for the case $p = q$, i.e. the symmetric XXZ chain with additional boundaries).

5. Toy model

In this chapter we study analytically a modified version of the Hamiltonian treated before. The results for different boundary conditions show that the main new features in comparison to the hermitian chain can already be found in this toy model. This model allows to understand which term in the Hamiltonian is responsible for the new and unexpected contributions to the spectrum.

We will concentrate on

$$H = \sum_{j=1}^{N-1} \sigma_j^+ \sigma_{j+1}^- + \alpha \sigma_1^- + \beta \sigma_N^+ \quad (5.1)$$

For $\alpha = 0$ or $\beta = 0$ the spectrum consists only of the N times degenerate eigenvalue zero. So the whole structure of the spectrum is caused by both boundary terms together.

This Hamiltonian can be diagonalized in terms of free fermions. Moreover $H(\alpha, \beta)$ can be transformed into $H(-\alpha, -\beta)$ by applying the transformation $\sigma^\pm \rightarrow -\sigma^\pm$. For $\alpha\beta > 0$ the characteristic properties of the spectra described previously are reproduced.

In order to write H in terms of free fermions, we have to obtain a bilinear expression in σ -matrices so that standard fermionisation techniques can be applied [36]. Technically, this can be achieved by appending one lattice site at each end of the chain, site 0 and site $N + 1$ [37]. The Hamiltonian then reads

$$H' = \sum_{j=1}^{N-1} \sigma_j^+ \sigma_{j+1}^- + \alpha \sigma_0^x \sigma_1^- + \beta \sigma_N^+ \sigma_{N+1}^x \quad (5.2)$$

As σ_0^x and σ_{N+1}^x commute with H' thus being constants of motion, the spectrum of H' decomposes into four sectors $(++, +-, -+, --)$ corresponding to the eigenvalues ± 1 of σ_0^x and σ_{N+1}^x . The eigenvectors of the extended Hamiltonian include those of H . Therefore we can obtain the eigenvectors of the original problem by projecting onto the $(++)$ -sector.

Defining new operators τ_j^+ and τ_j^- [38] by

$$\tau_j^+ = \left(\prod_{i<j} \sigma_i^z \right) \sigma_j^x, \quad \tau_j^- = \left(\prod_{i<j} \sigma_i^z \right) \sigma_j^y \quad (j = 0, \dots, N + 1) \quad (5.3)$$

that obey the anticommutation relations of a Clifford-algebra

$$\{\tau_i^\mu, \tau_j^\nu\} = 2\delta_{i,j}^{\mu,\nu} \quad (i, j = 0, \dots, N + 1; \mu, \nu = \pm 1). \quad (5.4)$$

one can rewrite H' as a bilinear expression in τ_j^+ and τ_j^-

$$H' = - \sum_{\mu, \nu = \pm 1} \sum_{j=1}^{N-1} A_j^{\mu, \nu} \tau_j^\mu \tau_{j+1}^\nu + B^{\mu, \nu} \tau_0^\mu \tau_1^\nu + C^{\mu, \nu} \tau_N^\mu \tau_{N+1}^\nu \quad (5.5)$$

with

$$B = \frac{\alpha}{2} \begin{pmatrix} 1 & i \\ 0 & 0 \end{pmatrix}, \quad A = \frac{1}{4} \begin{pmatrix} 1 & i \\ -i & 1 \end{pmatrix} \quad (0 < j < N) \quad , \quad C = \frac{\beta}{2} \begin{pmatrix} 0 & i \\ 0 & 1 \end{pmatrix}. \quad (5.6)$$

Here we chose as a basis

$$A = \begin{pmatrix} A^{--} & A^{-+} \\ A^{+-} & A^{++} \end{pmatrix} \quad . \quad (5.7)$$

Then a second linear transformation

$$T_n^\gamma = \sum_{j=0}^N \sum_{\mu=\pm 1} (\psi_n^\gamma)_j^\mu \tau_j^\mu \quad (\gamma = \pm 1) \quad (5.8)$$

with

$$\{T_i^\mu, T_j^\nu\} = 2\delta_{i,j}^{\mu,\nu} \quad (i, j = 0, \dots, N + 1; \mu, \nu = \pm 1). \quad (5.9)$$

yields

$$H' = \sum_{n=0}^{N+1} \Lambda_n i T_n^- T_n^+ \quad (5.10)$$

$$2\Lambda_{N+2-n} \approx \frac{2n-1}{2} \frac{\pi}{N} + i \left(1 + \frac{\ln(2\alpha\beta)}{N} \right) \quad \text{for} \quad k > \frac{\pi}{2}. \quad (5.19)$$

Up to now we always treated the chain where two additional sites, 0 and $N+1$ have been added to the starting Hamiltonian. We obtain the spectrum of the Hamiltonian without these sites by projection onto the sector where the σ -matrices acting on the additional sites have eigenvalue 1. It can be shown that the spectrum of H with respect to the ground state E_0 for large N is obtained for even N by combining only an odd number of fermions with energies $2\Lambda_n$ and for odd lattice lengths by combining an even number of fermions. The ground state of the system is found to be in the sector with odd lattice lengths.

For the normalization constant, one reads off directly $\xi = 1$.

We turn now to the determination of the partition function because this can be compared directly to previous results. Writing $\tilde{H} = \frac{N}{\pi}(H - E_0)$ and using the triple product identity [18] we obtain

$$\begin{aligned} \text{tr} z^{\tilde{H}} &= \prod_{n=1}^{\infty} (1 + z^{n-\frac{1}{2}} z^{ia}) (1 + z^{n-\frac{1}{2}} z^{-ia}) \\ &= \sum_{m \in \frac{Z}{2}}^{\infty} z^{2(m+i\frac{a}{2})^2 + \frac{a^2}{2}} \prod_{n=1}^{\infty} (1 - z^n)^{-1} \end{aligned} \quad (5.20)$$

with

$$\frac{a}{2} = x + yN, \quad x = \frac{\ln(2\alpha\beta)}{2\pi}, \quad y = \frac{1}{2\pi} \quad . \quad (5.21)$$

Here we obtain $m \in Z$ for odd lattice lengths and $m \in Z + \frac{1}{2}$ for even lattice lengths. Absorbing the term $\frac{a^2}{2}$ into the ground state energy, we get the following expression:

$$E'_0(N) = -\frac{N}{2\pi} - \frac{1}{\pi} - \frac{\pi}{24N} + o(N^{-2}) \quad . \quad (5.22)$$

This corresponds to a system with conformal charge $c = 1$. For the partition function we obtain

$$\mathcal{Z} = z^{\frac{1}{24}} \sum_{m \in \frac{Z}{2}}^{\infty} z^{2(m+i(x+Ny))^2} \prod_{n=1}^{\infty} (1 - z^n)^{-1} \quad . \quad (5.23)$$

This is exactly the same result we found for the more complicated model with $R^2 = 2$.

Comparing the partition function for the toy model with the ones for the open and for the periodic XXZ-chain given in the introduction, we get some insight into the nature of the different new terms in the partition function. For asymmetric XXZ-chains without periodic boundary conditions, we get the spectrum of a Coulomb gas with one kind of charges only. In the case of the completely open chain we get electrical charges, in the case of non-diagonal, non-hermitian chains we get only magnetic charges. These boundary conditions also give rise to an imaginary shift ix in the magnetic charges that also appears for the periodic chain with a real twist [15]. In our case x depends on α, β and the ratio p/q . The lattice length-dependent term yN appears for all non-hermitian chains we mentioned in this article except for the completely open chain which is equivalent to the hermitian symmetric open XXZ-chain.

6. Conclusions

In this article, the spectrum of the asymmetric XXZ-chain with non-hermitian boundary terms has been studied. Numerical methods have been applied for the determination of the eigenvalues. Analytically, we studied a toy model that reproduces the characteristic properties of the full Hamiltonian. In two different cases, we concluded that the boundary terms are responsible for the phase transitions of the Hamiltonian.

We studied first the ferromagnetic chain with $\alpha, \beta > 0$ that describes the time evolution of a reaction-diffusion system with asymmetric diffusion in the bulk and additional injection and extraction terms at the boundaries. For the completely asymmetric chain the behaviour of the smallest energy gap that corresponds directly to the inverse temporal correlation length shows the same behaviour as the spatial correlation length in the stationary state determined by [3]. In phases A and B where the spatial correlation length stays finite, i.e. the concentration of particles shows an exponential decay in the spatial direction, we find a massive spectrum where the mass depends on the same parameters as the spatial correlation length in the different phases A_1, A_2, B_1 and B_2 . In this way the subdivision of the phases A and B is also valid for the dynamical properties of H . However, the numerical values of the spatial and the temporal correlation lengths do not coincide. The phase C , where the spatial correlation length of the stationary state decays algebraically, exhibits a decay of the temporal correlation length with an exponent $\frac{3}{2}$. This exponent has already been identified for the model with periodic boundary conditions. On the coexistence line, we find a decay with an exponent 2. The deep reason why the phase diagram of the stationary state is reflected in the time-evolution of the system is not yet understood.

The antiferromagnetic chain for $\Delta < 1$ shows a completely different behaviour. For $\alpha = 0$ or $\beta = 0$ the spectrum corresponds to that of a XXZ-chain with additional σ^z -terms at the boundaries and therefore is massive. Only when both α and β are non-zero, the spectrum is massless and can be described by a representation of a non-unitary $U(1)$ Kac-Moody algebra. However, one term proportional to the lattice length arises in the finite-size scaling spectrum. The result can be summarized in the partition function of a modified Coulomb gas with only magnetic charges:

$$\mathcal{Z} = z^{-\frac{1}{24}} \sum_{m \in \frac{\mathbb{Z}}{2}} z^{R^2(m+i(x+Ny))^2} \Pi_V(z) \quad (6.1)$$

The parameters y and R also appear for periodical boundary conditions while x is induced by the boundary terms. The analysis of the toy model that was diagonalized in terms of free fermions reproduces the same structure of the spectrum. The length-dependent term seems to be a common property of the anisotropy of the spin chain [32] and also appeared for the periodic chain [8]. The imaginary shift of the magnetic charge is an effect of the non hermitian and non-diagonal boundary terms. The influence of hermitian boundary terms and asymmetric interactions in the bulk will be the subject of a future publication [39].

The question arises now how the ordinary Coulomb gas model has to be modified so that imaginary and lattice-length dependent contributions to the operator content arise. Is it still possible to find a field theory that reproduces the spectrum of the modified Coulomb gas? A first step in this direction could be the calculation of the correlation functions that normally, for conformal invariant systems, exhibit critical exponents which are directly related to the eigenvalues of the corresponding Hamiltonian. Whether this relation is still valid in the case of non-hermitian chains still has to be clarified.

The new and unexpectedly interesting structure that appeared in the two examples treated in this article suggests further research in the field of non-hermitian Hamiltonians.

Acknowledgements

We wish to thank Prof. V. Rittenberg for suggesting this interesting problem and for enlightening discussions and constant support. We are very grateful to Prof. D. Kim for valuable discussions and suggestions. We wish to thank the whole group for constant help and discussions.

References

- [1] Derrida B., Domany E. and Mukamel D. 1992 *J. Stat. Phys* **69** 667
- [2] Schütz G. and Domany E. 1993 *J. Stat. Phys.* **72** 277
- [3] Derrida B., Evans M.R., Hakim V. and Pasquier V. 1993 *J. Phys. A: Math. Gen.* **26** 1493
- [4] Sandow S. 1994 *Phys. Rev.* **E50** 2660
- [5] Essler H.L. and Rittenberg V. 1996 *J. Phys. A: Math. Gen.* **29** 3375
- [6] Gwa L. and Spohn H. 1992 *Phys. Rev. A* **46** 844
- [7] Kim D. 1995 *Phys. Rev. E* **52** 3512
- [8] Noh J.D. and Kim D. 1995 *Phys. Rev. E* **53** 3225
- [9] de Vega H.J. and Gonzales-Ruiz A. 1994 *J. Phys. A: Math. Gen.* **27** 6129; Inami T. and Konno H. 1994 *J. Phys. A: Math. Gen.* **27** L913
- [10] Kogut J.B. 1979 *Rev. Mod. Phys.* **51** 659
- [11] Sutherland B. 1967 *Phys. Rev. Lett.* **19** 103; Lieb E. and Wu F.Y. 1972 in *Phase Transitions and Critical Phenomena* Vol.1 (Academic Press: London)
- [12] van Beijeren H. 1977 *Phys. Rev. Lett.* **38** 993 ; Jayaprakash C. and Saam W.F. 1984 *Phys. Rev. B* **30** 3916; Jayaprakash C., Saam W.F. and Teitel S. 1983 *Phys. Rev. Lett.* **50** 2017; Bukman D.J. and Shore J.D. 1995 *J. Stat. Phys.* **78** 1277
- [13] see for example Krug J. and Spohn H. 1991 in *Solids far from equilibrium: growth, morphology and defects* edited by Godrèche C. (Cambridge University Press: Cambridge)
- [14] Albertini G., Dahmen S.R. and Wehefritz B. 1996 *J. Phys. A: Math. Gen.* **29** L369
- [15] Alcaraz F.C., Baake M., Grimm U. and Rittenberg V. 1988 *J. Phys. A: Math. Gen.* **21** L117
- [16] Alcaraz F.C., Barber M.N. and Batchelor M.T. 1987 *Phys. Rev. Lett.* **58** 771; Hamer C.J., Quispel G.R.W. and Batchelor M.T. 1987 *J. Phys. A: Math. Gen.* **20** 567 7; Alcaraz F.C., Barber M.N., Batchelor M.T., Baxter R.J. and Quispel G.R.W. 1987 *J. Phys. A: Math. Gen.* **20** 6397; Hamer C.J. and Batchelor M.T. 1988 *J. Phys. A: Math. Gen.* **21** L173; Alcaraz F.C., Barber M.N. and Batchelor M.T. 1988 *Ann. Phys* **182** 280; Alcaraz F.C. and Wreszinski W.F. 1990 *J. Stat. Phys* **58** 45
- [17] Di Francesco P., Saleur H. and Zuber I.-B. 1987 *Nucl. Phys. B* **285** 454; Nienhuis B. 1987 in *Phase Transitions and Critical Phenomena* Vol.11 (Academic Press: London)
- [18] Ginsparg P. 1988 in *Fields, Strings and Critical phenomena* Les Houches 1988 (North-Holland: Amsterdam)
- [19] Yildirim K. 1995 *Diplomarbeit*, BONN-IB-95-02
- [20] von Gehlen G. 1994 *Int. J. Mod. Phys.* **8** 3507
- [21] Kadanoff L.P. and Swift J. 1968 *Phys. Rev.* **165** 310
- [22] Pasquier V. and Saleur H. 1990 *Nucl. Phys. B* **330** 523
- [23] Saad Y. 1980 *Linear Algebra Appl.* **34** 269; Saad Y. 1981 *Math. Comp.* **37** 105; Saad Y. 1992 *Numerical Methods for Large Eigenvalue Problems* (Manchester University Press)
- [24] Burlisch R. and Stoer J. 1964 *Numer. Math.* **6** 413; Henkel M. and Schütz G. 1988 *J. Phys. A: Math. Gen.* **21** 2617
- [25] Neergard J. and den Nijs M. 1995 *Phys. Rev. Lett.* **74** 730
- [26] Kardar M., Parisi G. and Zhang Y.C. 1986 *Phys. Rev. Lett.* **56** 889
- [27] Alcaraz F.C., Droz M., Henkel M. and Rittenberg V. 1994 *Ann. Phys., NY* **230** 250
- [28] Blöte H.W.J., Cardy J.L. and Nightingale M.P. 1986 *Phys. Rev. Lett.* **56** 742
- [29] Affleck I. 1986 *Phys. Rev. Lett.* **56** 746
- [30] Cardy J.L. 1986 *Nucl. Phys. B* **270** 186

- [31] Cardy J.L. 1988 in *Fields, Strings and Critical Phenomena* Les Houches 1988 (North-Holland: Amsterdam)
- [32] Kim D. and Pearce P. 1987 *J. Phys. A: Math. Gen.* **20** L451
- [33] Dahmen S.R. and Wehefritz B. *unpublished*
- [34] Goddard P. and Olive D. 1986 *Int. J. Mod. Phys. A* **1** 303
- [35] Corrigan E. 1986 *Phys. Lett.* **169B** 259
- [36] Lieb E., Schultz T. and Mattis D. 1961 *Ann. Phys.* **16** 407
- [37] Hinrichsen H., Krebs K. and Peschel I. 1996 *Z. Phys.* **B100** 105
- [38] Hinrichsen H. 1994 *J. Phys. A: Math. Gen.* **27** 5393
- [39] Bilstein, U. and Wehefritz, B. *in preparation*

List of Figures

- 1 Phase diagram for the total asymmetric diffusion model 22

List of Tables

- I Asymmetric diffusion model: Dependence of the extrapolated gap E_G on α and β . 23
- II Asymmetric diffusion model: Extrapolated exponents of the first excited state. 24
- III Extrapolated and predicted values of the energy gaps, computed from the finite size spectrum of $-H$ for $\alpha = \beta = 0.5$, $q = 0$, $p = 1$ and $r = 0$. 24
- IV Like table III for $r \geq 0$ in the sectors $m = 0$ and $m = \frac{1}{2}$. 25
- V Dependence of the free surface energy f_∞ on α, β . 26
- VI Central charges for $\alpha = \beta$. 26
- VII Dependence of R^2x on α and β . 26

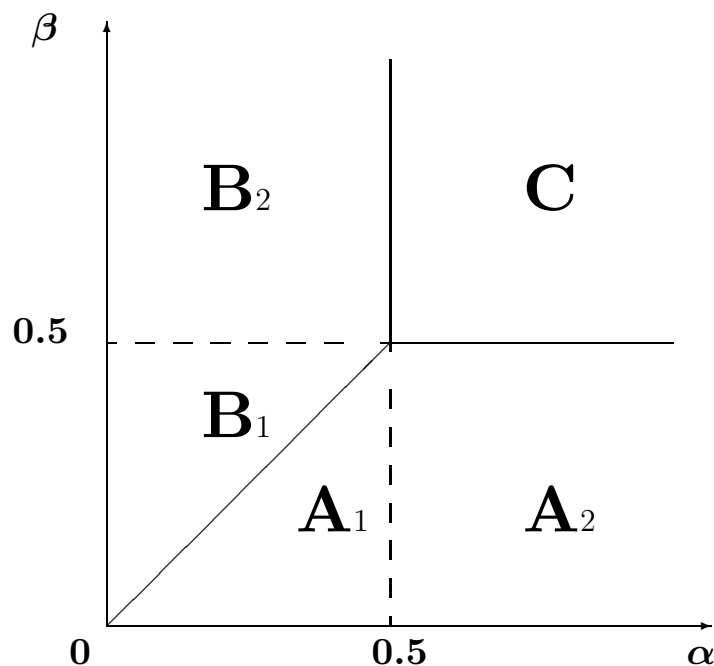


Figure 1. Phase diagram for the total asymmetric diffusion model

Table I. Asymmetric diffusion model: Dependence of the extrapolated gap E_G on α and β . Negative values indicate that errors are of the order of 10^{-5} .

$\beta \setminus \alpha$	0.1	0.2	0.3	0.4	0.5	0.6	0.7	0.8	0.9	1.0
1.0	0.12573	0.04014	0.01017	0.00119	0.00000	0.00001	-0.00002	-0.00001	-0.00000	0.00000
0.9	0.12575	0.04014	0.01021	0.00118	-0.00003	0.00000	-0.00004	-0.00001	-0.00000	
0.8	0.12573	0.04013	0.01019	0.00118	-0.00001	0.00000	-0.00004	-0.00004		
0.7	0.12587	0.04012	0.01019	0.00114	-0.00003	-0.00002	-0.00004			
0.6	0.12017	0.04016	0.01030	0.00120	-0.00001	-0.00001				
0.5	0.09999	0.03331	0.00861	0.00110	0.00000					
0.4	0.07213	0.02018	0.00330	-0.00005						
0.3	0.04173	0.00678	-0.00001							
0.2	0.01428	-0.00001								
0.1	-0.00000									

Table II. Asymmetric diffusion model: Extrapolated exponents of the first excited state.

$\beta \setminus \alpha$	0.1	0.2	0.3	0.4	0.5	0.6	0.7	0.8	0.9	1.0
1.0					1.5000	1.470	1.456	1.480	1.4999	1.522
0.9					1.499	1.452	1.503	1.4994	1.4999	
0.8					1.4997	1.430	1.436	1.499		
0.7					1.462	1.405	1.499			
0.6					1.434	1.377				
0.5					1.49999					
0.4				2.01						
0.3			1.98							
0.2		2.010								
0.1	1.992									

Table III. Extrapolated and predicted values of the energy gaps, computed from the finite size spectrum of $-H$ for $\alpha = \beta = 0.5$, $q = 0$, $p = 1$ and $r = 0$.

m	R^2m^2		$2R^2my$		$2R^2mx$
	prediction	extrapolated	prediction	extrapolated	extrapolated
$\frac{1}{2}$	0.317648	0.31763(2)	0.182104	0.182104	-0.12070(3)
1	1.270594	1.270(6)	0.364209	0.3642(1)	-0.2414(1)
$\frac{3}{2}$	2.858836	2.858(9)	0.546313	0.546313	-0.36210(7)
2	5.082375	5.082(3)	0.728418	0.728(4)	-0.4828(2)
$\frac{5}{2}$	7.941211	7.9(4)	0.910522	0.9(1)	-0.60(4)
3	11.435343	11.4(8)	1.092627	1.0(8)	-0.72(3)

Table IV. Data corresponding to (4.13) from the extrapolation of the spectra of $-H$ for $\alpha = \beta = 0.5$, $q = 0$, $p = 1$ with $2 \leq N \leq 21$; predicted degeneracies are given in square brackets; the predicted values of $2R^2mx$ are determined from the extrapolation of the value $2R^2mx$ for $m = \frac{1}{2}$ and $r = 0$.

		$m = 0$			$m = \frac{1}{2}$			
r	$R^2m^2 + r$	$2R^2mx$	$2R^2my$	r	$R^2m^2 + r$	$2R^2mx$	$2R^2my$	
1 [1]	1.000 000			0 [1]	0.317 63(2)	-0.120 70(3)	0.182 104	
2 [2]	1.999 99(7)	0.000 0(0)	0.000 00(1)	1 [1]	1.317 65(7)	-0.120 702	0.182 104	
3 [3]	3.000 0(0)			2 [2]	2.317 (4)	-0.120 (7)	0.182 1(1)	
	2.999 (8)	-0.000 (1)	-0.000 (0)		2.317 6(8)	-0.120 70(2)	0.182 104	
4 [5]	4.000 0(0)			3 [3]	3.3(2)	-0.12(0)	0.182 (1)	
	4.00(0)	0.000 (1)	-0.000 (0)		3.317 (7)	-0.120 7(0)	0.182 1(0)	
	4.0(0)	0.00(3)	-0.00(0)		3.31(7)	-0.120 6(8)	0.182 1(1)	
5 [7]	4.99(6)			4 [5]	4.3(2)	-0.1(3)	0.18(4)	
	5.00(0)	0.00(0)	0.000 (0)		4.31(8)	-0.120 (7)	0.182 (1)	
	5.0(0)	0.0(0)	-0.00(1)		4.317 (7)	-0.120 (8)	0.182 0(8)	
					4.31(6)	-0.12(2)	0.18(2)	
6	5.99(7)				4.31(7)	-0.11(8)	0.182 (0)	
	6.0(1)	0.0(0)	-0.00(1)	5 [7]	5.31(7)	-0.121 (4)	0.182 0(8)	
	6.0(0)	0.00(1)	-0.00(0)		5.317 4(8)	-0.120 (7)	0.182 (1)	
	6.0(0)	0.0(0)	-0.00(1)		5.31(4)	-0.12(2)	0.18(2)	
			5.31(7)		-0.12(1)	0.18(2)		
7	7.0(1)				5.3(2)	-0.1(3)	0.18(4)	
	6.99(9)	-0.0(0)	-0.000 (0)		5.3(2)	-0.11(5)	0.1(8)	
	7.0(1)	0.0(0)	-0.00(1)					
8	8.0(0)			6	6.3(1)	-0.11(7)	0.182 (1)	
	8.0(2)				6.3(4)	-0.1(1)	0.18(1)	
	8.0(1)	0.0(0)	-0.00(1)					
	8.(1)	0.(0)	-0.00(5)					
	8.0(1)	0.0(0)	-0.00(1)					
prediction	0.000 000+r	0.000 000	0.000 000		0.317 648+r	[-0.120 70]	0.1 82 104	

Table V. Dependence of the free surface energy f_∞ on α, β .

$\beta \setminus \alpha$	1.5	1.3	1.1	0.9	0.7	0.5	0.3
0.1	0.4959(9)	0.30(9)	0.123(1)	-0.06(4)	-0.25(6)	-0.4631(0)	-0.71(0)
0.3	0.9086(1)	0.722(0)	0.535(8)	0.348(6)	0.1564(6)	-0.050216(5)	
0.5	1.15624(0)	0.96957(1)	0.78344(0)	0.596234(5)	0.4040372		
0.7	1.362(8)	1.176(2)	0.9900(9)	0.8028(9)			
0.9	1.555(0)	1.368(4)	1.18(2)				
1.1	1.742(2)	1.555(6)					
1.3	1.928(3)						

Table VI. Extrapolated central charges. The value of R^2x is determined from E_0^1 .

$\alpha = \beta$	f_∞	R^2x	c	c'
0.1	-1.12(3)	0.793(8)	12.9(8)	1.0(8)
0.2	-0.6(2)	0.506(0)	5.8(3)	1.0(0)
0.3	-0.297(8)	0.3339(8)	3.1(1)	1.0(1)
0.4	-0.0336(9)	0.2126(4)	1.84(8)	0.99(4)
0.5	0.19737	0.1207(0)	1.2752(8)	1.0000(8)
0.6	0.40965	0.0486(5)	1.044(4)	0.999(7)
0.7	0.610(7)	-0.008(7)	1.00(0)	0.99(9)
0.8	0.8049(7)	-0.054(6)	1.04(8)	0.99(2)
0.9	1.1829(2)	-0.0913(7)	1.2(7)	1.1(2)
1.0	1.369(5)	-0.1(2)	1.3(8)	1.1(1)

Table VII. Dependence of R^2x on α and β .

$\beta \setminus \alpha$	1.5	1.3	1.1	0.9	0.7	0.5	0.3
0.1	-0.29(9)	-0.30(9)	-0.32(5)	-0.35(2)	-0.39(3)	-0.45900	-0.565(6)
0.3	-0.06(8)	-0.07(8)	-0.09(4)	-0.12(1)	-0.1(6)	-0.22735	
0.5	0.0379(7)	0.02806	0.01165	-0.01467	-0.05601		
0.7	0.102(5)	0.092(6)	0.076(2)	0.049(9)			
0.9	0.14(3)	0.13(3)	0.11(7)				
1.1	0.17(0)	0.16(0)					
1.3	0.18(6)						